TABLE I

ATTENTUATION MEASUREMENTS OF MODEL I INCLINE ATTENTUATOR

Component (Refer to Fig. 1)	Frequency in Mc	Average Value in db	Maximum Spread of Measurements in db
Model I attenuator	9,000	2.064	0.003
	9,375	2.022	0.004
	9,800	2.031	0.003
	10,250	2.068	0.002

TABLE II

ATTENUATION MEASUREMENTS OF TWO TYPES OF INCLINE ATTENUATORS MADE WITH CONVENTIONAL WAVEGUIDE COMPONENTS

Components (Refer to Fig. 3)	Frequency in Mc	Average Value in db	Maximum Spread of Measurements in db
Coupler and load	7,400	2.640	0.004
Two 10-db attenuators	9,000	20.223	0.005

TABLE III

ATTENUATION MEASUREMENTS OF CONVENTIONAL TWO SECTION WAVEGUIDE ATTENUATORS

Component	Frequency in Mc	Average Value in db	Maximum Spread of Measurements in db
Conventional two section waveguide attenuator	2,850	10.267	0 040
	3,950	19.789	0 032
	15,000	10.519	0.040
	24,000	20 305	0.023

tion, the input energy is the main waveguide section is coupled to a second section of waveguide, and then coupled back to the main section of waveguide by means of two separate sets of coupling holes. Matched terminations are placed at each end of the auxiliary section of waveguide. Also, two matched terminations are placed near the center portion of the main waveguide section. The terminations in the main waveguide section may be placed back to back as shown in Fig. 2(b), or for greater convenience in construction, the two terminations may be separated and mounted near an access opening as shown in Fig. 2(a).

Two inline attenuators which make use of the schemes proposed above can be fabricated from conventional microwave components. Two different types of inline attenuators made with conventional waveguide components are shown in Fig. 3. In Fig. 3(a), a conventional three-port directional coupler is shown with the side-arm port terminated in a matched load. In Fig. 3(b) two conventional "inline" attenuators are connected in series so that the two end ports are aligned with a common reference axis.[1]

Three proposed methods for changing a conventional "inline" attenuator to a true inline attenuator are shown in Fig. 4. All of these methods consist of providing a bend in the waveguide sections near the port end.[2]

An experimental model utilizing the design shown in Fig. 1 has been constructed, and calibration experiments are being performed to attempt to demonstrate improved operation of the true inline attenuator. Initial measurements made utilizing conventional waveguide components as suggested above indicate improvement in calibration results with the simplified calibration procedure.

Fig. 5 shows a curve of the frequency characteristics of the Model I attenuator which is illustrated in Fig. 1. The calibration data are shown in Table I. Also, the calibration data taken at 7400 Mc with a directional coupler terminated in a matched load and at 9000 Mc with two conventional "inline" attenuators connected in series are shown in Table II. In order to compare the repeatability of measurement of these true inline attenuators, calibration data taken at several frequencies with conventional "inline" attenuators are shown in Table III. It is noted that the maximum spread of measurements in decibels is about an order of magnitude less for the true inline attenuators than for the conventional "inline" attenuators.

WILBUR LARSON
Radio Standards Lab.
Nat'l Bur. Standards
Boulder, Colo.

High-Speed Microwave Switches Using Silver-Bonded Diodes in the 11-Gc Region

This communication describes a high-speed microwave switch with a switching time as small as 0.5 nsec in the 11-Gc region. It employes silver-bonded diodes which have been originally developed as variable capacitance elements for use in parametric amplifiers.[1]

Several types of diode are illustrated in Table I.

These diodes were inserted in the diode mount illustrated in Fig. 1(a) in order to be examined as transmission-type switches. The isolation characteristics were adjusted to optimum by controlling the variable short in the short coaxial line. The average static switching characteristics were

1) insertion loss of about 1 db
2) isolation as large as 20 db
3) handling power as large as 100 mw
4) required controlling voltage of about 5 v

when good GSB2, SiSBR, SiSBY were used. The switching mode is "ON" in the case of forward bias and "OFF" in the case of reverse bias. Small numbers of diodes had an isolation as large as 40 db.

The transient waveforms of switched microwaves were observed with a wide-band synchronous detector and a sampling oscilloscope. The over-all amplitude rise time of the observation system was smaller than 0.5 nsec.[2] The quadrature component was much smaller than the in-phase component. Therefore it was sufficient for our purposes to observe only the latter one. The diode was supplied with a negative static bias voltage and a positive rectangular pulse with rise and fall times of about 0.3 nsec.

The observed amplitude rise and fall times (10–90 per cent value in the in-phase component) were

0.5–0.75 nsec (without any overshoot and undershoot),

0.4 nsec (with overshoot and undershoot as large as 20 per cent)

in the case of nonconducting switches for any type of silver-bonded diode. "Conducting" or "nonconducting" means that the over-all bias voltage (static bias plus pulse) drives the diode; conducting or not conducting, respectively.

In some cases conducting switches are desirable because of their shaping effect. In fact, the flat-top rectangular microwave nanosecond pulse cannot be generated without the conducting switch, since the applied baseband nanosecond pulse always has a variety of waveform distortions.

The switching rise time is independent of the condition of conducting. On the other hand, the fall time is largely affected by it.

Fig. 2(a) illustrates the fall time of transmission-type switches as a function of the applied pulse voltage for the four types of silver-bonded diodes, where the applied pulse voltage means the incident pulse voltage in the coaxial line of 50 ohms. We concluded from the measurements of diode transient current that the deteriorated fall time is due to the hole storage effect.

Reflection-type switches were also examined. The construction is illustrated in Fig. 1(b). The static forward bias current and the negative pulse were applied to the diode, and the switched microwave signal was observed. The switching rise time was largely affected by the static bias current as illustrated in Fig. 2(b). These results also show

Manuscript received March 7, 1963; revised February 10, 1964.

[1] Conversation with G. E. Schafer, Chief, Div. 92, Nat'l Bur. Standards, Boulder, Colo.
[2] Conversation with R. W. Beatty, Consultant, Nat'l Bur. Standards, Boulder, Colo.

[1] S. Kita, T. Okajima and M. Chung, "Parametric amplifier using a silver bonded diode," IRE TRANS. ON ELECTRON DEVICES, vol. ED-8, pp. 105–109; March, 1961.

[2] K. Miyauchi, "Observations of nanosecond Carrier pulses," IEEE TRANS. ON MICROWAVE THEORY AND TECHNIQUES, vol. MTT-12, pp. 221–230; March, 1964.

TABLE I

Type	Material	Specific Resistance (ohm-cm)	Holder	Commercial or Experimental
GSB1	Ge	0.05	1N263 Type	Commercial
GSB2	Ge	0.1	1N263 Type	Commercial
SiSBR	Si	0.03	1N263 Type	Experimental
SiSBV	Si	0.1–0.08	1N263 Type	Experimental

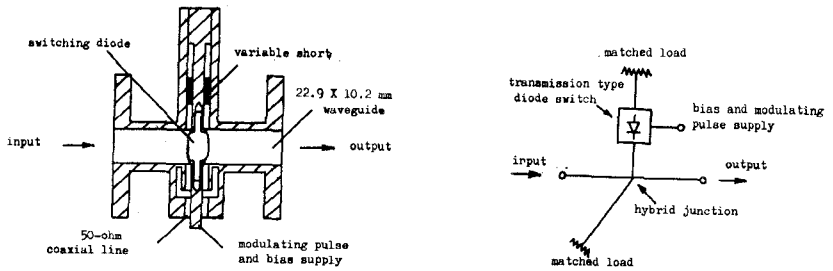

Fig. 1—Construction of diode switches.

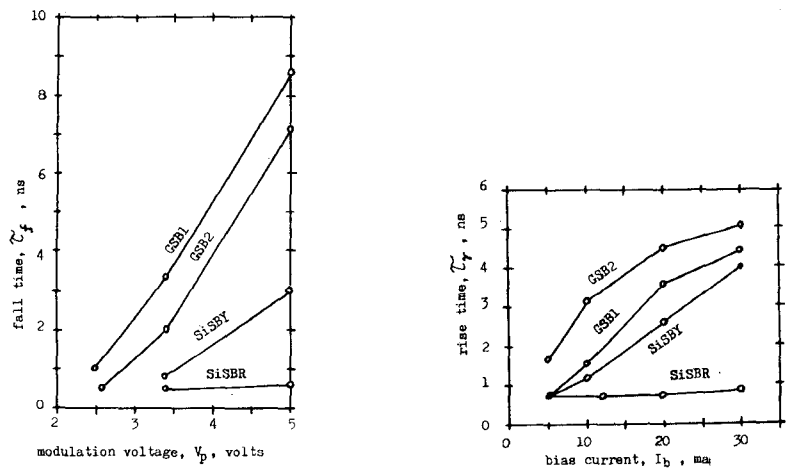

Fig. 2—Rise and fall times of diode switches in the conducting case. (a) Transmission type (microwave input power = 5 mw, static bias voltage = −5 v). (b) Reflection type (microwave input power = 5 mw, applied pulse voltage = 2 v).

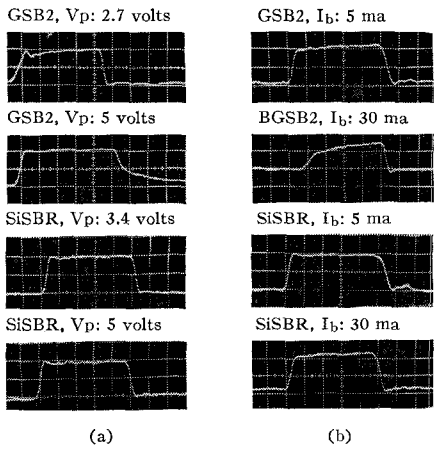

Fig. 3—Microwave pulse waveforms (in-phase components) of diode switch output. V_p = applied pulse voltage, I_b = static bias current, horizontal axis = 2 nsec/div. (a) Transmission type (microwave input power = 5 mw, static bias voltage = −5 v). (b) Reflection type (microwave input power = 5 mw, applied pulse voltage = 2 v).

the hole storage effect. The switching fall time was almost independent of the static bias current and was about 0.5–0.7 nsec.

Fig. 3 illustrates the typical waveforms (in-phase components) of switched microwave pulses when the GSB2 and SiSB diodes are applied with a rectangular pulse of 20 nsec in the transmission and reflection-type switches.

It was concluded that the silicon silver-bonded diode SiSBR has the best rise and fall times: about 0.5 nsec.

Acknowledgment

The authors wish to thank Dr. B. Oguchi and Dr. S. Kita for their helpful discussions, and R. V. Garver for his encouragement.

Kazuhiro Miyauchi
Osamu Ueda
Electrical Communication Lab.
Tokyo, Japan

Addendum to "An Exact Method for Synthesis of Microwave Band-Stop Filters"

Summary

An algorithm is presented that enables a designer to compute efficiently and quickly the design parameters of microwave band-stop filters that are based on the exact synthesis technique previously discussed by Schiffman and Matthaei. Tables of band-stop filter designs that give maximally flat and Chebyshev responses are presented for ten typical stop-band fractional bandwidths.

Introduction

By extending work of Ozaki and Ishii [1], Schiffman and Matthaei [2], [3] have presented a theory and several design equations for an exact method of synthesizing microwave band-stop filters. Using their synthesis procedure, a band-stop filter is developed from a low-pass, lumped-element prototype filter. The band-stop filter is composed of either quarter-wavelength short-circuited stubs connected in series with the main transmission line, or quarter-wavelength open-circuited stubs connected in shunt with the main transmission line. The stubs are spaced at either quarter- or three-quarter-wavelengths. The characteristic immittances of the stubs and connecting lines depend on the low-pass filter that is used as a prototype. If the low-pass prototype filter has an attenuation function $L_A(\omega'/\omega_1')$, the band-stop filter will have a response $L_A\{\Lambda \tan [(\pi/2)(\omega/\omega_0)]$ where L_A is the transducer attenuation in decibels. The arguments of the attenuation function L_A are defined as follows:

- ω' is the frequency variable of the low-pass prototype filter,
- ω_1' is the cutoff frequency of the low-pass prototype filter,
- ω is the frequency variable of the band-stop filter,
- ω_0 is the center frequency of the band-stop filter,
- Λ is a scaling parameter that is defined

$$\Lambda = \omega_1' \tan [(\pi/4)w]. \quad (1)$$

The symbol w in (1) is the fractional stop bandwidth of the band-stop filter. It is defined by

$$w = \frac{\omega_2 - \omega_1}{\omega_0}, \quad (2)$$

where ω_2 and ω_1 are the cutoff frequencies of the band-stop filter corresponding to ω_1' of the low-pass prototype filter.

Figs. 1(a) and 1(b) show configurations of the low-pass prototype filter used in the synthesis procedure. Note that the parameters g_i of the prototype filter are also defined in Figs. 1(a) and 1(b). Figs. 1(c) and 1(d) show typical maximally flat and Chebyshev responses of the filters of Figs. 1(a) and 1(b), respectively. Tables of g_i

Manuscript received December 9, 1963. This work was sponsored by the U. S. Army Electronics Research and Development Laboratory, Fort Monmouth, N. J., under Contract No. DA 36-039-AMC-00084(E).